TRANSPORTES
revistatransportes.org.br
anpet
associação nacional de pesquisa e ensino em transportes
anpet.org.br

Advancements and applications of X-ray micro-computed tomography and digital image processing for the characterization of asphaltic materials

Avanços e aplicações da microtomografia computadorizada de raios X e do processamento digital de imagens na caracterização de materiais asfálticos

Thiago Delgado de Souza[1], Alexis Jair Enríquez-León[1], Francisco Thiago Sacramento Aragão[1], André Maués Brabo Pereira[2], Liebert Parreiras Nogueira[3]

[1]Federal University of Rio de Janeiro, Rio de Janeiro, Rio de Janeiro – Brasil
[2]Fluminense Federal University, Niterói, Rio de Janeiro – Brasil
[3]University of Oslo, Oslo – Norway

contato: engthiagodelgado@gmail.com, (TDS); aenriquez.eng@gmail.com, (AJEL); fthiago@coc.ufrj.br, (FTSA); andre@ic.uff.br, (AMBP); l.p.nogueira@odont.uio.no, (LPN)

Submitted:
04 October, 2022
Accepted for publication:
16 January, 2023
Published:
3 May, 2023

Editor in charge:
Jorge Barbosa Soares

Keywords:
X-ray micro-computed tomography.
Digital image processing.
Asphaltic materials.
Artificial intelligence.

Palavras-chave:
Microtomografia computadorizada de raios X.
Processamento digital de imagens.
Materiais asfálticos.
Inteligência artificial.

DOI: 10.58922/transportes.v31i1.2854

ABSTRACT
This paper presents recent advances of the application of the X-ray microtomography (micro-CT) technique in the characterization of asphaltic materials. Imaging characteristics to perform micro-CT tests of asphalt concrete and fine aggregate matrix mixtures are discussed. A procedure developed to perform the digital image processing of the asphaltic materials images is also presented. The key findings from this paper are: (1) spatial resolutions between 10 µm/pixel and 13 µm/pixel are adequate to perform the evaluation of asphaltic material volumetrics; (2) instead of thresholding, the U-Net architecture can be used to optimize the digital image processing; (3) a representative volume element comprising 33% of the sample volume can be adopted for volumetric evaluations of asphaltic materials; (4) fine aggregate matrix volumetric properties are dependent on the asphalt mixture volumetrics.

RESUMO
Este artigo apresenta os avanços recentes da aplicação da técnica de microtomografia computadorizada de raios X (micro-TC) na caracterização de materiais asfálticos. São discutidas as características de aquisição das imagens para realizar ensaios de micro-TC de concretos asfálticos e matrizes de agregados finos. Um procedimento desenvolvido para realizar o processamento digital das imagens dos materiais asfálticos também é apresentado. As principais conclusões deste artigo são: (1) resoluções espaciais entre 10 µm/*pixel* e 13 µm/*pixel* são adequadas para realizar a avaliação da volumetria dos materiais asfálticos; (2) em vez da limiarização, a arquitetura *U-Net* pode ser utilizada para otimizar o processamento digital de imagens; (3) um elemento de volume representativo considerando 33% do volume total das amostras pode ser adotado para avaliações da volumetria de materiais asfálticos; (4) a volumetria da matriz de agregados finos é dependente da volumetria da mistura asfáltica correspondente.

1. INTRODUCTION

Asphalt mixtures are composite materials comprising aggregates, air voids (AVs), and asphalt binders. The volumetric composition, the characteristics, and the interaction among such constituents play a key role on the performance of the surface layer of flexible pavements. Thus, the development and application of research methods that allow the characterization of these materials is essential for the understanding of their complex behavior.

The X-ray computed tomography (CT) is one of the non-destructive methods to characterize the microstructure of asphaltic materials. It is a technique that allows the acquisition of images for the visualization and characterization of morphological parameters of their constituents. CT has been adopted in different fields, including material science, botany, diagnostic medicine, zoology, geology, soils, and electronics (Enríquez-León et al., 2022).

The inherent heterogeneity of composite materials makes the use of CT adequate, given that their constituents present varying density and chemical composition, which results in distinct abilities to absorb radiation. This difference in the absorption and attenuation of the waves is the key for the acquisition of CT images (Reis Neto et al., 2011).

CT is based on the X-ray attenuation equation, described by the Lambert-Beer Law, which indicates that the intensity of a beam of monochromatic light decreases exponentially as the thickness of the absorbing medium increases arithmetically (Augusto, 2016). In the process, a source emits a photon beam with intensity I_0 and these X-rays pass through the object. The interaction between the photons and the elements that constitute the objects attenuates the intensity of the X-rays, which leave the object with a smaller intensity, I, which is then measured by the detector (Palombo, 2017). After that acquisition of the projections, the sections of the object are reconstructed, which leads to the generation of two-dimensional digital images. Those may in turn compose a three-dimensional image.

A digital image is composed by a group of pixels (picture elements). The pixel is the smallest unit of the digital image. Such an image is a matrix in which each element is a number representing the color or the intensity of the pixel in the corresponding position of the real image (Gonzales and Woods, 2010). In three-dimensional images, the units are named as voxels, a neologism created from the combination of the words volume and pixels. The voxels correspond to the pixels and to their depth.

In a digital image, the spatial resolution describes the smallest portion of the image that can be captured, i.e., it indicates the smallest distance between two distinct points. The resolution is taken as the inverse of the real size of the pixel (pixel size). It is a key parameter in CT characterizations, as it is related to different features of the system, including: i) distance between the X-ray source and the detector from the sample; ii) binning; and iii) optical magnification with the aid of lenses. Thus, the resolution should be carefully evaluated t guarantee representative results for the object of interest.

This research effort presents a systematic literature review using the bibliometrix tool (Aria and Cuccurullo, 2017) and focusing on the Web of Science database. Using combinations and Boolean operators of the type Topic, 20 papers were found. The search considered title, abstract, and keywords, and was made according to the description (((TS=(*x-ray computed tomography*)) AND TS=(*asphalt concrete mixtures*)) AND TS=(*digital image processing*)). After the compilation of the obtained information, the manuscripts were manually evaluated to differentiate TC and micro-TC efforts. The snowball selection method (Goodman, 1961) was also adopted.

Some authors have used CT to evaluate the microstructure of asphalt materials (Sadeq et al., 2018; Shaheen, Al-Mayah and Tighe, 2016; Thyagarajan et al., 2010; You, Adhikari and Emin Kutay, 2008; Tashman et al., 2002; Masad et al., 1999; 2002). The study carried out by Masad et al. (1999) identified the distribution of AVs in laboratory and field specimens. In samples produced in the laboratory with low compaction energies, the distribution of air voids was more homogeneous, mainly in the central region of the samples. In the case of field samples, the AVs decreased with the depth of the asphalt surface layer. These results were corroborated in the study by Tashman et al. (2002), in which the distribution of air voids was more uniform on the horizontal axis than on the vertical axis. Another AV distribution study was carried out by Thyagarajan et al. (2010). It was found that the use of saws to trim the samples reduces the vertical heterogeneity, but does not influence the horizontal heterogeneity.

In Brazil, Nascimento et al. (2006) used CT to evaluate the AV distribution of laboratory-compacted samples considering Marshall and Superpave procedures. They also analyzed specimens obtained in the field and concluded that the extraction of cores is not necessary to perform testing with cylindrical specimens of asphalt mixtures.

Although important observation about the characteristics of air voids within asphalt mixture samples could be drawn from these studies that adopted CT procedures, the pixel size and the image segmentation were limiting factors to obtain more conclusive results. Underwood (2011) indicated that the limitation resulting from the spatial resolution may generate results that are not representative, given that resolutions around 310 μm/*pixel* are not sufficient to identify and characterize most of fines and fillers.

Considering that asphalt mixtures generally contain micrometric particles in their composition, it may be necessary to adopt more robust techniques such as the X-ray microcomputed tomography (micro-CT). The micro-CT is similar to the CT, but produces images in three dimensions with spatial resolutions near one micrometer (Landis and Keane, 2010). Recent research on the microstructural characteristics of asphalt concretes (ACs) and fine aggregate matrices (FAMs) from micro-CT images have adopted distinct resolutions, as shown in Table 1.

Table 1: Resolutions of micro-CT images adopted by different researchers

Author	Resolution (μm/pixel)
Enríquez-León et al. (2021)	3.0
Souza et al. (2022)	6.0
Enríquez-León et al. (2021; 2022)	7.0
Amelian et al. (2019), Osmari et al. (2020)	7.8
Hu et al. (2015), Hu et al. (2017), Souza et al. (2022)	10.0
Enríquez-León et al. (2021)	13.0
Enríquez-León et al. (2021), Chen et al. (2022)	14.0
Souza et al. (2022)	20.0
Enríquez-León et al. (2021)	22.0
Zhao et al. (2021)	28.7
Zhang et al. (2015)	40.0
Onifade et al. (2013)	59.0
Onifade and Birgisson (2016)	59.0
Wang et al. (2018)	60.0
Sun et al. (2022)	78.0
Liu et al. (2018), Kollmann et al. (2019a; 2019b)	80.0

Although some authors have demonstrated the potential of the micro-CT for the microstructural characterization of ACs, additional studies are required to define a procedure for the selection of parameters that are adopted in these tests. Additionally, several simplifications are often adopted in the digital image processing (DIP) step, which follows the tomography tests. This may compromise the accuracy of the results, as the images are generally not treated and segmented with procedures that allow to minimize the dependence of the DIP operator skills on the reproducibility of the results.

The use of artificial intelligence (AI) in the DIP is a good alternative to automatize the analysis procedure (Yang et al., 2022; Enríquez-León et al., 2022; Jiang et al., 2018). However, depending on the sample dimensions, the procedures may present a prohibitive high cost and require a significant computational effort. Thus, analyses considering the representative volume element (RVE) should be conducted to identify the sample dimensions that can provide results that represent the global characteristics of the material (Al-Raoush and Papadopoulos, 2010).

This paper presents recent advancements in the application of the micro-CT technique for the characterization asphaltic materials. Several aspects are discussed, including spatial resolutions, DIP, and RVE for ACs and FAMs. A recently developed procedure to perform the DIP is presented. Finally, the relationship between volumetric characteristics of ACs and FAMs identified from micro-CT analyses is also analyzed.

2. MICRO-CT OF ASPHALTIC MATERIALS

Figure 1 illustrates the steps for the acquisition and analysis of images of an asphalt mixture using micro-CT. The reconstruction of the images considering slices of the object of interest is based on the direction of the X-rays that cross the samples in distinct trajectories (Travincas et al., 2023).

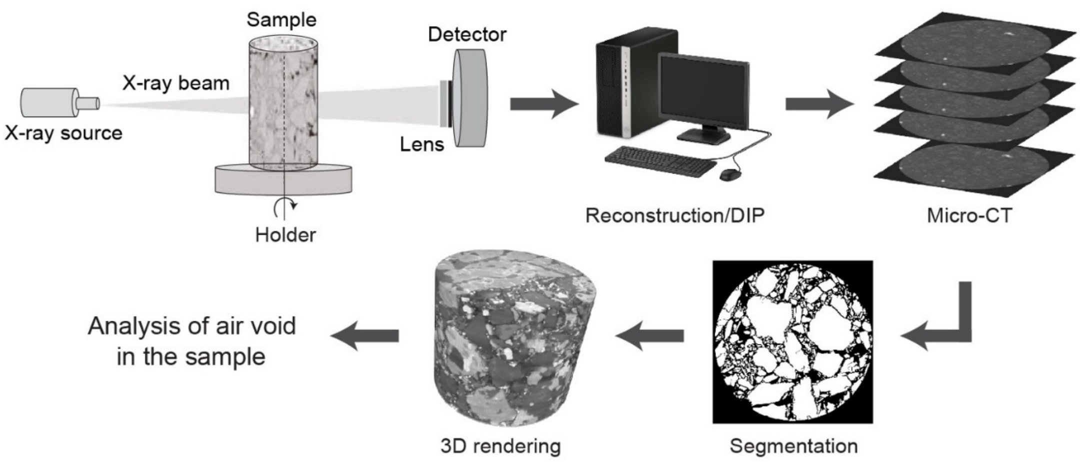

Figure 1. Illustration of the micro-CT process adopted to quantify the microstructural characteristics of asphaltic materials (adapted from Zelelew et al., 2013 and Tashman et al., 2002)

2.1. Micro-CT image resolution of asphaltic materials

In a digital image, the unit of the spatial resolution is distance by number of pixels (Gomes, 2007). This resolution is a key parameter in micro-CT analyses and must be carefully evaluated to guarantee good results. As an example, Osmari et al. (2020) and Amelian et al. (2019) adopted a resolution of 7.8 μm/pixel. Figure 2 exemplifies the effect of the spatial resolution on the quality of micro-CT images.

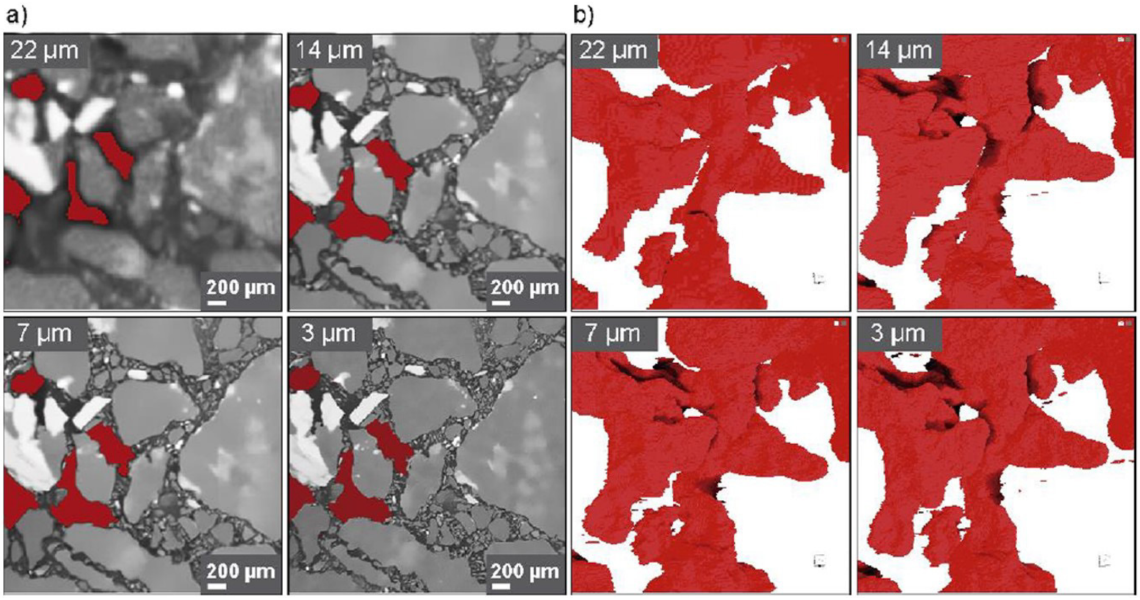

Figure 2. Effect of the spatial resolution on the characterization of AVs:
a) cross sections and b) 3D rendered images

Enríquez-León et al. (2021) evaluated the microstructural air void characteristics of ACs considering different spatial resolutions, i.e., 3 μm/pixel, 7 μm/pixel, 14 μm/pixel, and 22 μm/pixel, as illustrated in Figure 3. The maximum variation among the resolutions of 3 μm/pixel, 7 μm/pixel, and 14 μm/pixel was 3.5%. When compared to the other resolutions, the results for 22 μm/pixel presented a maximum variation of 8.1%. This result was corroborated by other tests considering resolutions of 7 μm/pixel and 13 μm/pixel, for which the maximum variation was 1.9%. Based on these results, 13 μm/pixel was selected as an adequate spatial resolution for AC characterizations.

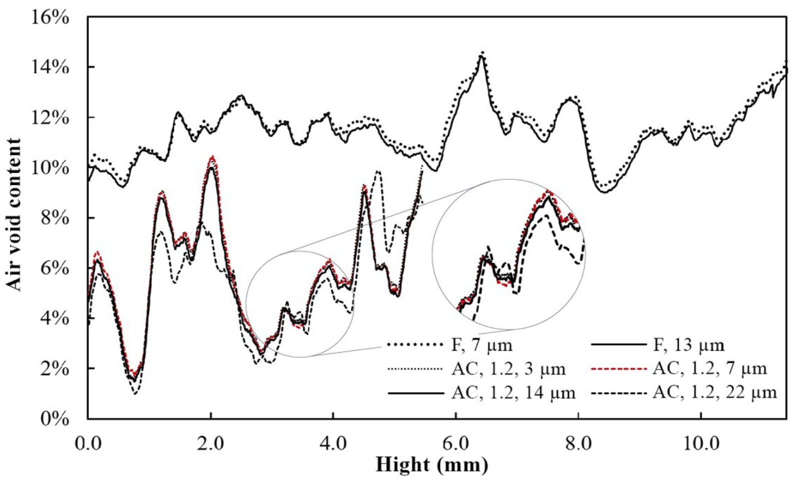

Figure 3. Characterization of AVs using different spatial resolutions in an AC sample (Enríquez-León et al., 2021)

Souza et al. (2022) adopted three resolutions for the microstructural characterization of air voids in FAMs, i.e., 6 μm/pixel, 10 μm/pixel, and 20 μm/pixel. The maximum variation between the resolutions of 6 μm/pixel and 10 μm/pixel was 2.5%. When compared to the other resolutions, the 20 μm/pixel resolution presented a maximum variation of 19.9%. Thus, 10 μm/pixel was selected as adequate to characterize the AV content in FAMs.

3. DIP OF ASPHALTIC MATERIALS

Du Plessis and Boshoff (2019) evaluated that the analysis of micro-CT images is cumbersome and involves complex procedures. It may be significantly affected by the skills of the operator if thresholds are manually selected in the segmentation process. Thus, it is necessary to advance on the development and application of automatic and standard analysis procedures.

DIP is a key step for the acquisition of microstructural characteristics of the materials. It can be divided in three parts: pre-processing, segmentation, and post-processing.

After evaluating several images of asphaltic materials, Souza et al. (2022; 2023), Enríquez-Léon et al. (2021; 2022), and observed that the pre-processing involves two main steps: histogram equalization and application of the *Non-Local Means Denoising* (NLM) filter (Buades et al., 2011). Figure 4b illustrates the histogram equalization of an image to evenly redistribute the intensity values of the pixels in an AC sample. With the use of this tool, the amount of pixels is similar for any gray shade and the image histograms become more uniform. The NLM filter reduces the noise of the image without compromising the quality in the borders. With that filter, the peaks are better defined in the post-application histogram, as shown in Figure 4c.

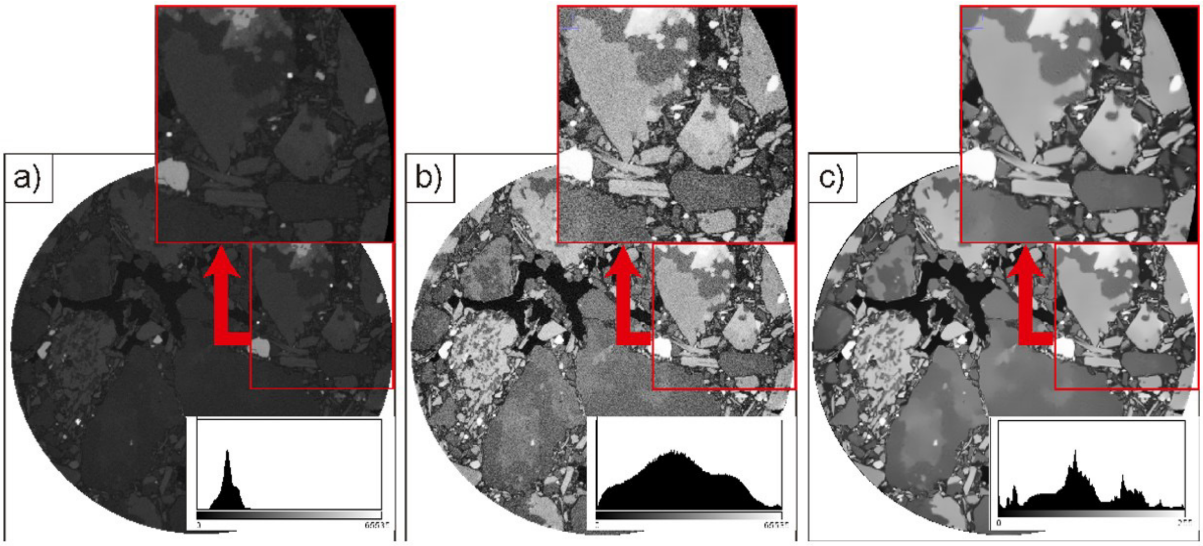

Figure 4. Example of pre-processing: a) original micro-CT image, b) pre-processed image with equalization, and c) pre-processed image with NLM filter

Figure 5 presents an example of an image after pre-processing in which two AC phases can be identified: aggregates and mastic in gray, and AVs in black. To identify pixels and quantify the AVs or other constituents, it is necessary to segment the images.

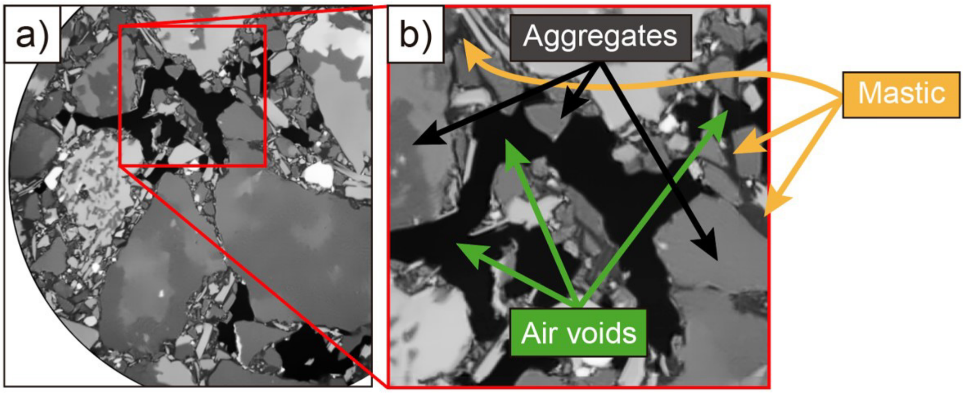

Figure 5. AC constituents: a) original image and b) amplified image

During the segmentation, the gray shade of the pixels is used to differentiate the material constituents and generate a binary image. In the analysis of the image histogram, a threshold is identified. The pixels with gray shade below that threshold are converted to white and the remaining pixels are converted to black, or vice-versa (Gomes, 2007).

To perform the DIP segmentation, a variety of techniques may be employed. The most common, known as threshold (TH), is limited, given that the definition of the threshold depends on the skills of the operator, on the homogeneity of the images, and on the complexity of the material. Thus, it is hard to guarantee the reproducibility in this process. Figure 6 presents variations on the AVs in the AC sample segmented considering four different TH values.

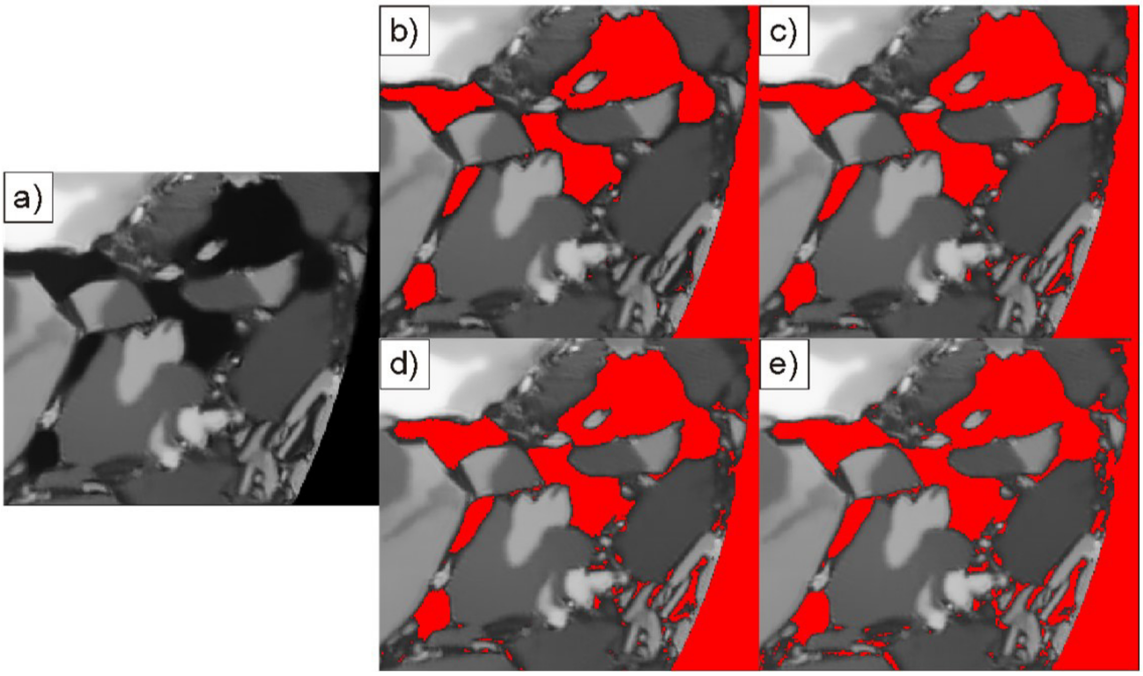

Figure 6. Application of TH in an AC image: a) original, b) with TH of 30, c) with TH of 35, d) with TH of 40, and e) with TH of 45

One of the main limitations of TH is the sensibility of the results. Within the selected range in the example above, i.e., TH between 30 and 45, the average of AVs was between 4.11% and 8.32%, as shown in Figure 7. This represents a relative error of 51% and highlights the importance of the study of other segmentation techniques to provide more accurate results.

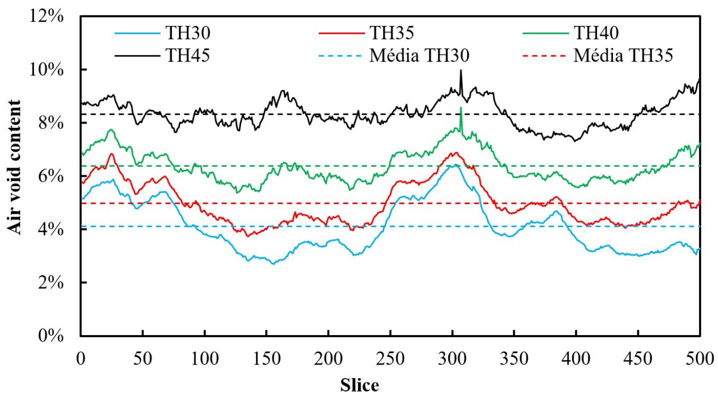

Figure 7. Distribution of AVs in an AC sample for different TH values

New techniques developed within the field of AI, such as machine learning and deep learning, have emerged as promising alternatives to improve the reproducibility and efficiency of processing times (Yang et al., 2022; Enríquez-León et al., 2022; and Jiang et al., 2018). According to Bezerra et al. (2020), AI can be applied to DIP and offer optimization for segmentation, as it allows training only a few slices or sections of the sample, generating a pattern recognition that can be replicated in the entire sample or in new samples that have similar characteristics. Although humans are more competent than computers in recognition tasks, AI techniques are capable of making the segmentation process much faster and more reproducible, which is extremely difficult with the use of the TH technique due to the complexity of the microstructure of asphalt materials.

AI techniques use computer programs such as Fiji/ImageJ (Schindelin et al., 2012) and Dragonfly (Provencher, Piché and Marsh, 2019; ORS, 2020). With these programs, it is possible to train neural networks to identify air voids, minimizing operator-related effects accurately. The efforts by Souza et al. (2022) and Enríquez-Léon et al. (2022) suggest that the U-Net architecture has been successful in segmenting micro-CT images of asphalt materials, as shown in Figure 8.

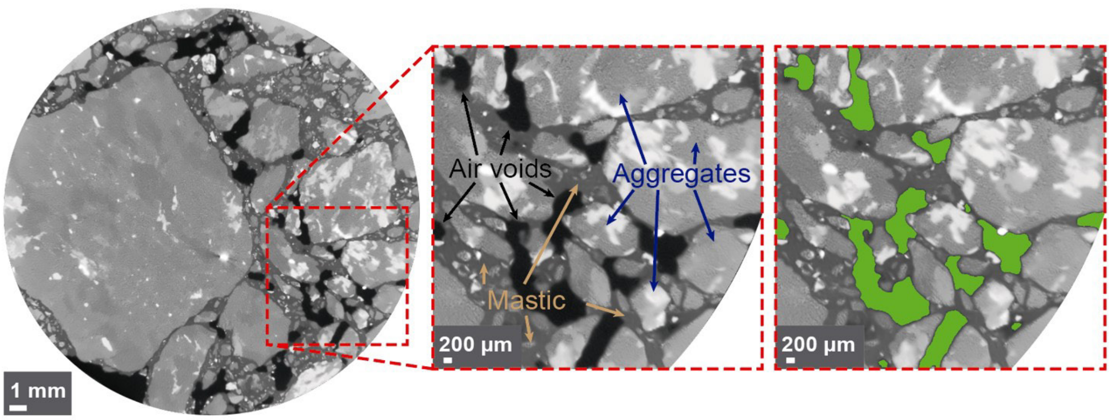

Figure 8. Segmentation of AVs in AC using the U-Net architecture (Enríquez-Léon et al., 2021)

After segmentation, some computational operations are required in post-processing to correct possible noises that may occur during the acquisition of micro-CT images. The first operation that may be necessary for post-processing is stitching to join the micro-CT images of a specimen to create unique specimens. Other morphological operations must also be applied, including filling in internal areas and removing insignificant air voids, which are actually noises with tiny dimensions when compared to other AVs. Then, the samples can be rendered in three dimensions. Three-dimensional rendering consists of generating virtual images representing the real object as the final result of the DIP.

4. RVE OF ASPHALT MATERIALS

The RVE can be defined as a minimum volume for which the measurable macroscopic characteristics of a porous medium remain constant. This means that for a given volume, the variations of the measured properties of a sample are minimized to the point of reaching a stability plateau (Al-Raoush and Papadopoulos, 2010).

Table 2 and Figure 9 present the candidate cylindrical geometries for RVE selected to perform the characterization of AVs in AC. In turn, Table 3 and Figure 10 present the candidate cylindrical geometries for RVE selected to characterize FAM AV contents.

Table 2: Candidate geometries for RVE of AC

ID of the tentative RVE	Percentage of the height of the AC sample	Percentage of the diameter of the AC sample
A	100	100
B	75	100
C	50	100
D	33	100
E	25	100
F	100	50
G	75	50
H	50	50
I	33	50
J	25	50

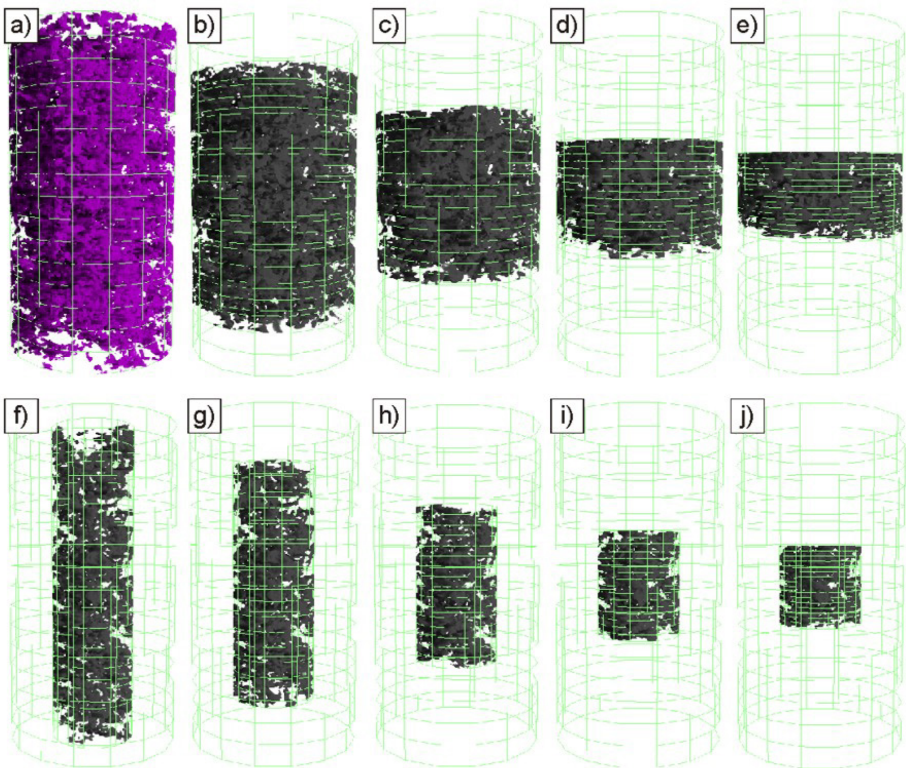

Figure 9. Candidate geometries for RVE of AC (Enríquez-Léon et al., 2021)

Table 3: Candidate geometries for RVE of FAM

ID of the tentative RVE	Percentage of the height of the FAM sample	Percentage of the diameter of the FAM sample
A	100	100
B	67	100
C	50	100
D	33	100
E	100	50
F	67	50
G	50	50
H	33	50

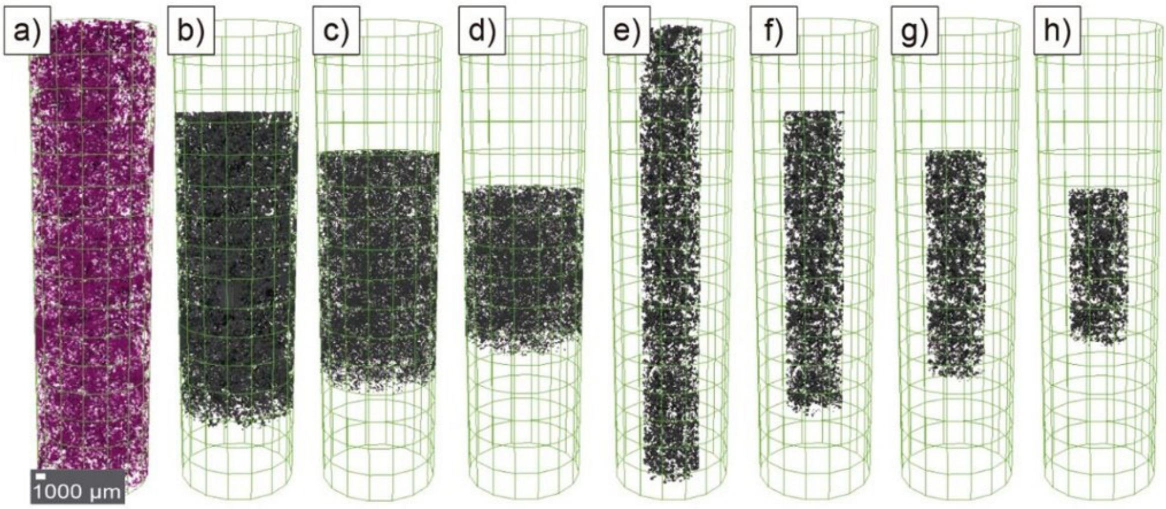

Figure 10. Candidate geometries for RVE of FAM (Souza et al., 2022)

Candidate geometries of cylindrical RVEs with volumes larger than 33% of the volumes of the corresponding original specimens showed minor differences in air void content compared to the original samples. Thus, the tentative RVE with 33% of the testing specimen volume (Figures 10d and 11d) was the most optimized, allowing for a balance between the practicality of image acquisition and its adequate representativeness. This means that the central third portion makes a good reproduction of the total AVs of the FAM and AC specimens. This information is essential to reduce micro-CT and DIP time and computational costs. It is worth noting that this RVE was defined for volumetric analyses. RVEs for other characteristics, such as mechanical behavior, should be evaluated in future work.

5. RESULTS OF MICRO-CT APPLICATION IN VOLUMETRIC EVALUATIONS OF ASPHALT MATERIALS

This section compiles the experience of the authors and several results from micro-CT applications to evaluate asphalt materials in a single analysis (Souza et al., 2022; 2023; Enríquez-León et al., 2021; 2022). Based on these research efforts, it may be concluded that micro-CT is an adequate technique to measure the air void content of FAMs and ACs. As shown in Figure 11, a good correspondence was observed with the laboratory conventional method (LCM), which consists of determining the maximum and bulk specific gravities of asphalt mixture samples to calculate their air void content (Souza et al., 2022; Enríquez-León et al., 2021).

The total air voids (total AVs) obtained from micro-CT can be subdivided into two groups, open and closed AV (Bruker, 2020). Open air voids are connected to the sample outer surface and are assumed to be permeable. Closed air voids, on the other hand, do not interact with the external surface, so they are theoretically impermeable (Enríquez-León et al., 2022).

Asphalt mixtures (samples A to G) with higher air void content also showed a higher percentage of open air voids, identifying a strong correlation with the LCM, as seen in Figure 12. For the FAM (sample H), this correlation did not apply, as closed AV had a higher percentage than open AV. This fact can be attributed to the characteristic size of the air voids, since in the FAM the air voids were much smaller than in the AC. However, the results of FAM total AVs obtained from micro-CT (2.98%) and MCL (2.90%) were very similar.

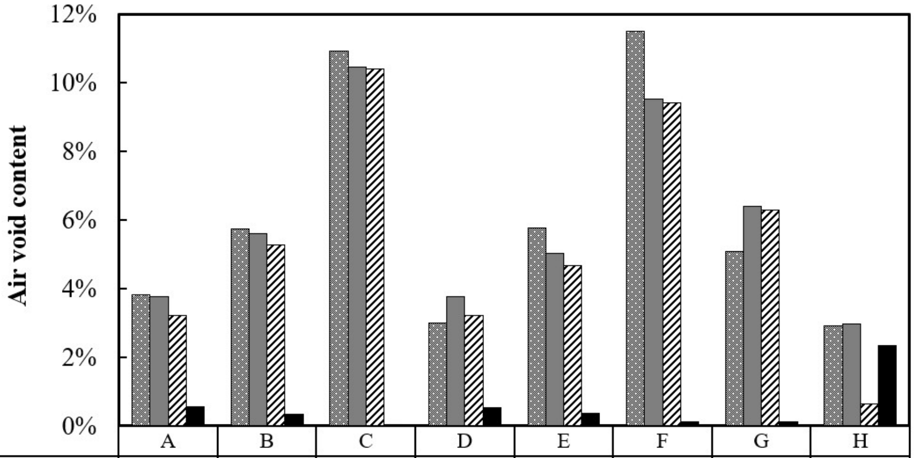

	A	B	C	D	E	F	G	H
LCM	3,82%	5,74%	10,92%	3,00%	5,76%	11,50%	5,07%	2,90%
Micro-CT (total AV)	3,76%	5,59%	10,45%	3,75%	5,04%	9,53%	6,39%	2,98%
Open AV	3,22%	5,27%	10,41%	3,22%	4,66%	9,42%	6,28%	0,64%
Closed AV	0,55%	0,33%	0,04%	0,54%	0,37%	0,12%	0,11%	2,34%

Identification of samples

Figure 11. Comparison between air void contents obtained by different methods for ACs and FAMs (Souza et al., 2022 and Enríquez-León et al., 2021)

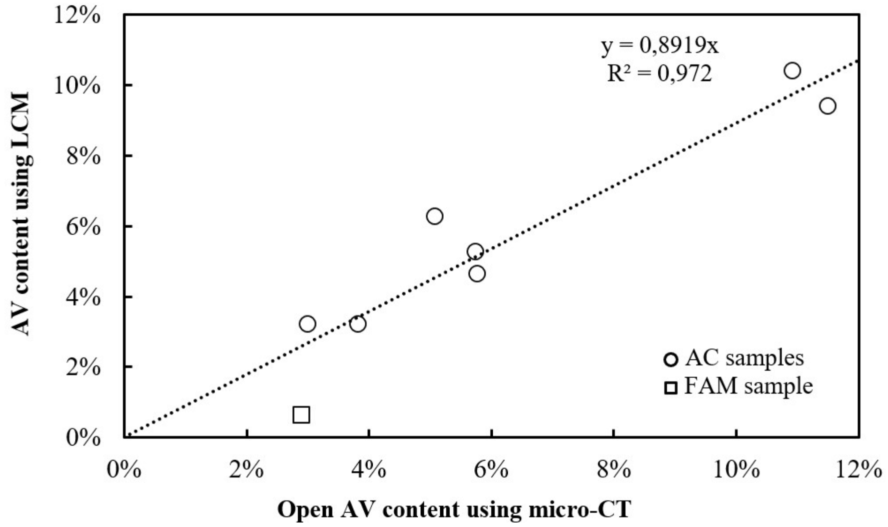

Figure 12. Correlation between open AV content obtained by micro-CT and LCM (Souza et al., 2022 and Enríquez-León et al., 2021)

After identifying micro-CT as a suitable technique to quantify air voids in ACs and FAMs, Enríquez-León et al. (2021) developed a methodology to determine the air voids belonging to the FAM phase within the ACs, considering the interaction between the AVs and the aggregates as a criterion for classifying types of air voids, as illustrated in Figure 13. Thus, the air voids that touched the coarse aggregate particles were excluded from the images.

An envelope was implemented around each aggregate particle to determine the interaction limit between air voids and aggregates, whose thickness varied between 0 µm and 150 µm. Then, the group of resulting images was visually evaluated to identify which values eliminated the air voids touching the coarse aggregates. The 150-µm envelope eliminated all AVs touching the coarse aggregates. The FAM AV was between 18.5% and 36.1% of the total AV in the corresponding AC mixtures. Furthermore, a strong correlation was identified between air voids in AC and its corresponding FAM, as illustrated in Figure 14. This correlation can be helpful in the fabrication of FAM samples with volumetric characteristics similar to those of FAMs that compose the corresponding ACs (Enríquez-León et al., 2021).

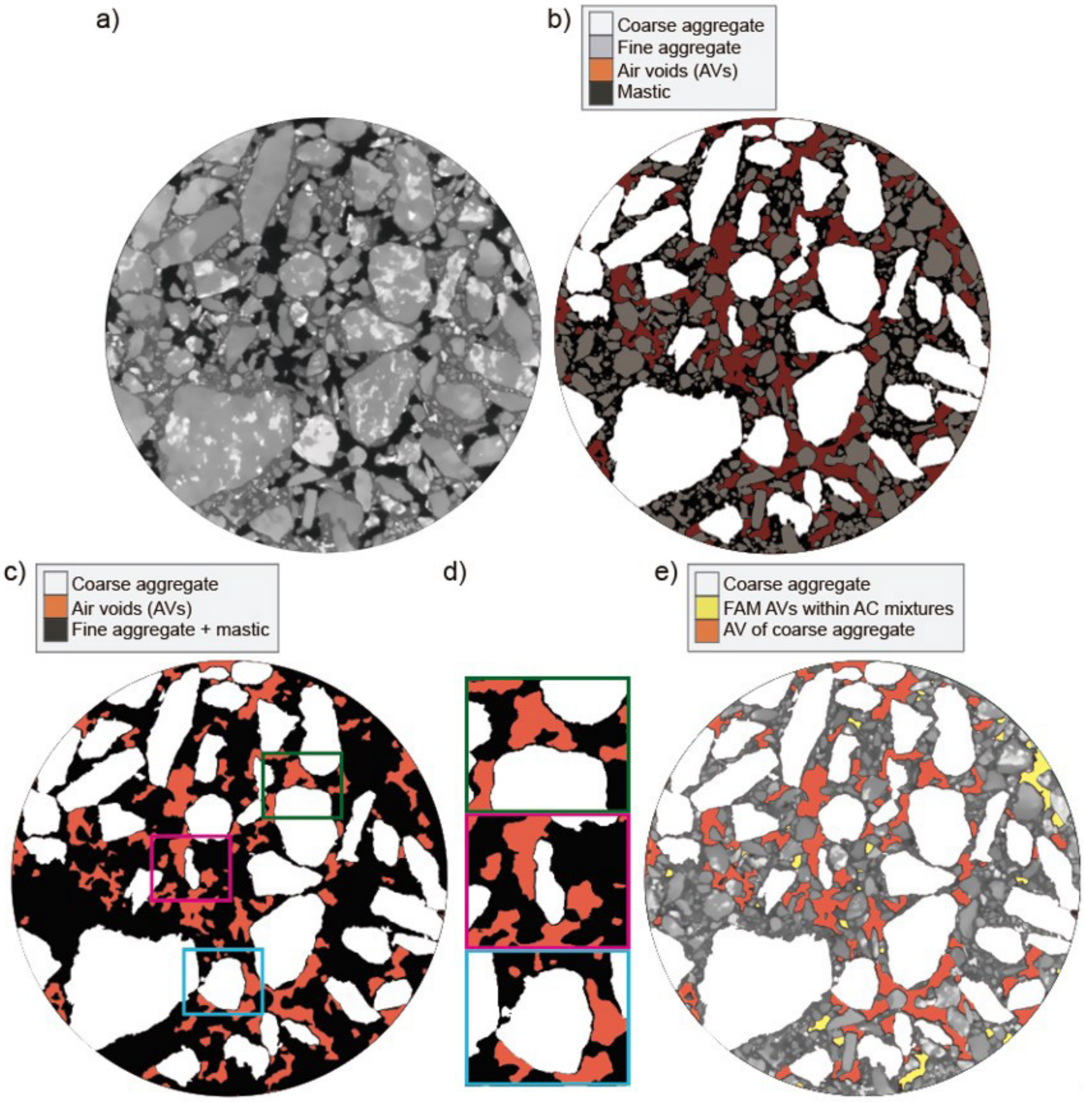

Figure 13. a) Cross section image of an AC, b) segmented image of coarse aggregates, fine aggregates, AVs, and mastic, c) AVs around coarse aggregates particles, d) details of AVs touching coarse aggregates, and e) different types of AVs in the microstructure of the AC

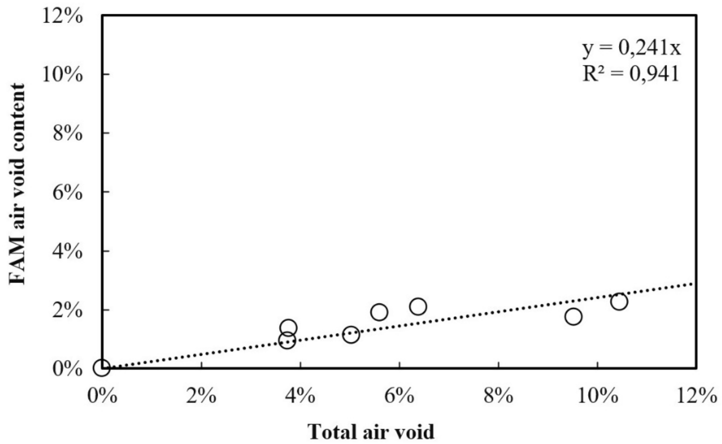

Figure 14. Correlation between total AC AV and FAM AV contents

6. SUMMARY AND CONCLUSIONS

This article presents recent advancements in the characterization of asphalt materials using the X-ray microtomography (micro-CT). Appropriate resolutions and representative volume element (RVE) were identified for micro-CT testing of these composites. In addition, a digital image processing (DIP) procedure recently developed by the authors and results from the application of micro-CT in volumetric evaluations of asphalt materials were presented. The main conclusions are indicated below.

- Resolutions of 10 to 13 μm/pixel were identified as suitable for performing micro-CT of asphalt materials.
- The U-Net convolutional neural network proved a powerful tool for segmenting images of asphalt materials acquired from micro-CT.
- The representative volume element (RVE) for volumetric analysis of asphalt materials was characterized as the central third portion of the samples, which represents 33% of their total volume. Additional studies should be carried out to characterize RVEs for other properties of asphalt materials, such as stiffness, moisture-induced damage, fatigue, and permanent deformation.
- The determination of air voids (AVs) by micro-CT and the laboratory conventional method (LCM) showed a high correlation, indicating that both methods can quantify the air voids of asphalt materials. LCM is recommended for expedited analyses, while micro-CT is recommended for detailed evaluations of asphalt materials.
- The AVs in the fine aggregate matrix (FAM) is strongly correlated with the AVs of the corresponding asphalt concrete (AC), that is, for the manufacture of isolated FAMs, the volumetry of the corresponding AC must be considered.

ACKNOWLEDGEMENTS

This study was financed by the Coordenação de Aperfeiçoamento de Pessoal de Nível Superior - Brasil (CAPES) - Código de Financiamento 001, by the Conselho Nacional de Desenvolvimento Científico e Tecnológico (CNPq), and by the Fundação de Amparo à Pesquisa do Estado do Rio de Janeiro (FAPERJ).

REFERENCES

Al-Raoush, R. and A. Papadopoulos (2010) Representative elementary volume analysis of porous media using X-ray computed tomography. *Powder Technology*, v. 200, n. 1-2, p. 69-77. DOI: 10.1016/j.powtec.2010.02.011.

Amelian, S.; Y.R. Kim; P.H. Osmari et al. (2019) Development of a volumetric mix design approach for fine aggregate matrix (FAM) and validation with micro-CT method. In *Transportation Research Board 98th Annual Meeting*. Washington, D. C., Estados Unidos.

Aria, M. and C. Cuccurullo (2017) Bibliometrix: an R-tool for comprehensive science mapping analysis. *Journal of Informetrics*, v. 11, n. 4, p. 959-75. DOI: 10.1016/j.joi.2017.08.007.

Augusto, K. (2016) *Microtomografia Computadorizada de Raios X Aplicada à Caracterização de Porosidade em Pelotas de Minério de Ferro*. Tese (doutorado). PUC-Rio, Rio de Janeiro. Available at: <https://www.maxwell.vrac.puc-rio.br/colecao.php?strSecao=resultado&nrSeq=29701@1> (accessed 10/04/2022).

Bezerra, E.; K. Augusto and S. Paciornik (2020) Discrimination of pores and cracks in iron ore pellets using deep learning neural networks. *REM - International Engineering Journal*, v. 73, n. 2, p. 197-203. DOI: 10.1590/0370-44672019730119.

Bruker (2020) CTAnalyzer v. 1.20.3 [Computer Software]. Kontich, Belgium. Available at: <https://www.bruker.com/en/products-and-solutions/preclinical-imaging/micro-ct/3d-suite-software.html> (accessed 10/04/2022).

Buades, A.; B. Coll and J.-M. Morel (2011) Non-local means denoising. *Image Processing On Line Journal*, v. 1, p. 208-12. DOI: 10.5201/ipol.2011.bcm_nlm.

Chen, A.; G.D. Airey; N. Thom et al. (2022) Characterisation of fatigue damage in asphalt mixtures using X-ray computed tomography. *Road Materials and Pavement Design*. In press. DOI: 10.1080/14680629.2022.2146601.

Du Plessis, A. and W.P. Boshoff (2019) A review of X-ray computed tomography of concrete and asphalt construction materials, *Construction & Building Materials*, v. 199, p. 637-51. DOI: 10.1016/j.conbuildmat.2018.12.049.

Enríquez-León, A.J.; T.D. Souza; F.T.S. Aragão et al. (2021) Characterization of the air void content of fine aggregate matrices within asphalt concrete mixtures. *Construction & Building Materials*, v. 300, p. 124214. DOI: 10.1016/j.conbuildmat.2021.124214.

Enríquez-León, A.J.; T.D. Souza; F.T.S. Aragão et al. (2022) Determination of the Air Void Content of Asphalt Concrete Mixtures using Artificial Intelligence Techniques to Segment Micro-CT Images, *The International Journal of Pavement Engineering*, v. 23, n. 11, p. 3973-82. DOI: 10.1080/10298436.2021.1931197.

Gomes, O.D.M. (2007) *Microscopia Co-Localizada: Novas Possibilidades na Caracterização de Minério*s. Tese (doutorado). PUC-Rio, Rio de Janeiro. Available at: <https://www.maxwell.vrac.puc-rio.br/colecao.php?strSecao=especifico&nrSeq=11498@1> (accessed 10/04/2022).

Gonzales, R.C. and R.E. Woods (2010) *Processamento Digital de Imagens* (3ª ed.). São Paulo: Pearson Prentice Hall.

Goodman, L.A. (1961) Snowball sampling. *Annals of Mathematical Statistics*, v. 32, n. 1, p. 148-70. DOI: 10.1214/aoms/1177705148.

Hu, J.; Z. Qian; Y. Liu et al. (2015) High-temperature failure in asphalt mixtures using micro-structural investigation and image analysis. *Construction & Building Materials*, v. 84, p. 136-45. DOI: 10.1016/j.conbuildmat.2014.12.090.

Hu, J.; Z. Qian; Y. Liu et al. (2017) Microstructural characteristics of asphalt concrete with different gradations by X-ray CT. *Journal of Wuhan University of Technology-Mater*, v. 32, n. 3, p. 625-32. DOI: 10.1007/s11595-017-1644-4.

Jiang, J.; Z. Zhang; Q. Dong et al. (2018) Characterization and identification of asphalt mixtures based on convolutional neural network methods using X-ray scanning images. *Construction & Building Materials*, v. 174, p. 72-80. DOI: 10.1016/j.conbuildmat.2018.04.083.

Kollmann, J.; G. Lu; P. Liu et al. (2019b) Parameter optimisation of a 2D finite element model to investigate the microstructural fracture behaviour of asphalt mixtures. *Theoretical and Applied Fracture Mechanics*, v. 103, p. 102319. DOI: 10.1016/j.tafmec.2019.102319.

Kollmann, J.; P. Liu; G. Lu et al. (2019a) Investigation of the microstructural fracture behaviour of asphalt mixtures using the finite element method, *Construction & Building Materials*, v. 227, p. 117078-91. DOI: 10.1016/j.conbuildmat.2019.117078.

Landis, E. and D. Keane (2010) X-ray microtomography. *Materials Characterization*, v. 61, n. 12, p. 1305-16. DOI: 10.1016/j.matchar.2010.09.012.

Liu, P.; J. Hu; H. Wang et al. (2018) Influence of temperature on the mechanical response of asphalt mixtures using microstructural analysis and finite-element simulations. *Journal of Materials in Civil Engineering*, v. 30, n. 12, p. 04018327. DOI: 10.1061/(ASCE)MT.1943-5533.0002531.

Masad, E.; B. Muhunthan; N. Shashidhar et al. (1999) Quantifying laboratory compaction effects on the internal structure of asphalt concrete. *Transportation Research Record: Journal of the Transportation Research Board*, v. 1681, n. 1, p. 179-85. DOI: 10.3141/1681-21.

Masad, E.; V.K. Jandhyala; N. Dasgupta et al. (2002) Characterization of Air Void Distribution in Asphalt Mixes using X-ray Computed Tomography, *Journal of Materials in Civil Engineering*, v. 14, n. 2, p. 122-9. DOI: 10.1061/(ASCE)0899-1561(2002)14:2(122).

Nascimento, L.; L. Leite; E. F. Campos et al. (2006) Uso da tomografia computadorizada e de imagens digitais para o estudo de misturas asfálticas. In *Anais do Encontro do Asfalto IBP - 18*. Rio de Janeiro.

Object Research Systems Inc. - ORS. (2020) Dragonfly 2020.1 [Computer Software]. Montreal, Canadá. Available at: <http://www.theobjects.com/dragonfly> (accessed 10/04/2022).

Onifade, I. and B. Birgisson (2016) Investigation of energy-based crack initiation threshold from meso-scale asphalt concrete response. In *8th RILEM International Conference on Mechanisms of Cracking and Debonding in Pavements*. Dordrecht: Springer, p. 679-85. DOI: 10.1007/978-94-024-0867-6_95.

Onifade, I.; D. Jelagin; A. Guarin et al. (2013) Asphalt internal structure characterization with X-ray computed tomography and digital image processing. In Kringos, N., B. Birgisson, D. Frost and L. Wang (eds) *Multi-Scale Modeling and Characterization of Infrastructure Materials*. Dordrecht: Springer, p. 139-58. DOI: 10.1007/978-94-007-6878-9_11.

Osmari, P.H.; R.F. Costa; F.T.S. Aragão et al. (2020) Determination of volumetric characteristics of FAM mixtures using X-ray micro-computed tomography and their effects on the rheological behavior of the material. *Transportation Research Record: Journal of the Transportation Research Board*, v. 2674, n. 5, p. 97-107. DOI: 10.1177/0361198120914607.

Palombo, L. (2017) *A Microtomografia de Raios X e a Porosimetria por Intrusão de Mercúrio na Determinação de Porosidade e Densidade de Rochas Reservatório*. Dissertação (mestrado). Universidade de São Paulo, São Paulo. DOI: 10.11606/D.3.2017.tde-11042017-140904

Provencher, B.; N. Piché and M. Marsh (2019) Simplifying and streamlining large-scale materials image processing with wizard-driven and scalable deep learning. *Microscopy and Microanalysis*, v. 25, n. S2, p. 402-3. DOI: 10.1017/S1431927619002745.

Reis Neto, J.; A. Fiori; A. Lopes et al. (2011) A microtomografia computadorizada de raios X integrada à petrografia no estudo tridimensional de porosidade em rochas. *Revista Brasileira de Geociencias*, v. 41, n. 3, p. 498-508. DOI: 10.25249/0375-7536.2011413498508.

Sadeq, M.; E.A. Masad; H. Al-Khalid et al. (2018) Characterisation of air voids in W-FAM samples using X-Ray CT imaging. In Masad, E., A. Bhasin, T. Scarpas, I. Menapace and A. Kumar (eds.) *Advances in Materials and Pavement Performance Prediction*. London: CRC Press, p. 97-100. DOI: 10.1201/9780429457791-25.

Schindelin, J.; I. Arganda-Carreras; E. Frise et al. (2012) Fiji: an open-source platform for biological-image analysis. *Nature Methods*, v. 9, n. 7, p. 676-82. DOI: 10.1038/nmeth.2019. PMid:22743772.

Shaheen, M.; A. Al-Mayah and S. Tighe (2016) A novel method for evaluating hot mix asphalt fatigue damage: X-ray computed tomography. *Construction & Building Materials*, v. 113, p. 121-33. DOI: 10.1016/j.conbuildmat.2016.03.030.

Souza, T.D.; A.J. Enríquez-León; C.R.R. Souza et al. (2022) Avaliação das características volumétricas de matrizes de agregados finos usando microtomografia e segmentação por Deep Learning. In *XXXVI ANPET*. Fortaleza.

Souza, T.D.; A.J. Enríquez-León; M.L. Rocha et al. (2023) A criterion to select the maximum aggregate size of fine-aggregate asphalt matrices. In *102nd Annual Meeting of the Transportation Research Board (TRB)*. Washington, D.C. DOI: 10.1177/03611981231159891.

Sun, Y.; Z. Zhang; H. Gong et al. (2022) 3D multiscale modeling of asphalt pavement responses under coupled temperature-stress fields. *Journal of Engineering Mechanics*, v. 148, n. 3, p. 1-15. DOI: 10.1061/(ASCE)EM.1943-7889.0002089.

Tashman, L.; E. Masad; J. D'Angelo et al. (2002) X-ray tomography to characterize air void distribution in superpave gyratory compacted specimens. *The International Journal of Pavement Engineering*, v. 3, n. 1, p. 19-28. DOI: 10.1080/10298430290029902a.

Thyagarajan, S.; L. Tashman; E. Masad et al. (2010) The heterogeneity and mechanical response of hot mix asphalt laboratory specimens. *The International Journal of Pavement Engineering*, v. 11, n. 2, p. 107-21. DOI: 10.1080/10298430902730521.

Travincas, R.; C.M.P. Manuel; I. Torres et al. (2023) X-ray microtomography applied to mortars: Review of microstructural visualization and parametrization. *Micron*, v. 164, p. 103375. DOI: 10.1016/j.micron.2022.103375. PMid:36334385.

Underwood, B.S. (2011) *Multiscale Constitutive Modeling of Asphalt Concrete*. Tese (doutorado). North Carolina State University, Carolina do Norte. Available at: <www.lib.ncsu.edu/resolver/1840.16/7217> (accessed 10/04/2022).

Wang, H.; C. Wang; Z. You et al. (2018) Characterising the asphalt concrete fracture performance from X-ray CT Imaging and finite element modelling. *The International Journal of Pavement Engineering*, v. 19, n. 3, p. 307-18. DOI: 10.1080/10298436.2017.1347440.

Yang, H.; J. Huyan; T. Ma et al. (2022) Novel computer tomography image enhancement deep neural networks for asphalt mixtures. *Construction & Building Materials*, v. 352, p. 129067. DOI: 10.1016/j.conbuildmat.2022.129067.

You, Z.; S. Adhikari and M. Emin Kutay (2008) Dynamic modulus simulation of the asphalt concrete using the x-ray computed tomography images. *Materials and Structures*, v. 42, n. 5, p. 617-30. DOI: 10.1617/s11527-008-9408-4.

Zelelew, H.M.; A. Almuntashri; S. Agaian et al. (2013) An improved image processing technique for asphalt concrete X-ray CT images. *Road Materials and Pavement Design*, v. 14, n. 2, p. 341-59. DOI: 10.1080/14680629.2013.794370.

Zhang, Y.; W. Verwaal; M.F.C. Van de Ven et al. (2015) Using high-resolution industrial CT scan to detect the distribution of rejuvenation products in porous asphalt concrete, *Construction & Building Materials*, v. 100, p. 1-10. DOI: 10.1016/j.conbuildmat.2015.09.064.

Zhao, Z.; J. Jiang; F. Ni et al. (2021) 3D-Reconstruction and characterization of the pore microstructure within the asphalt FAM using the X-ray micro-computed tomography, *Construction & Building Materials*, v. 272, p. 121764. DOI: 10.1016/j.conbuildmat.2020.121764.